Infrared Spectroscopy of Neat Solid Ozone and That of Ozone in Interaction with Amorphous and Crystalline Water Ice

H. Chaabouni, L. Schriver-Mazzuoli,* and A. Schriver

Laboratoire de Physique Moléculaire et Applications,† Unité propre du CNRS, Université Pierre et Marie Curie, Tour 13, case 76, 4 place Jussieu, 75252 Paris Cedex 05, France

Received: March 2, 2000; In Final Form: May 22, 2000

The interaction of ozone with ice films under high vacuum was studied with single reflection Fourier transform infrared spectroscopy (incidence angle of 5°). Both amorphous and crystalline ice were investigated. On amorphous ice which has a high density of free surface OH groups two states of ozone were observed: one which forms a hydrogen bond with the ice surface of the micropores, and a second which is attributed to a physisorbed state. Only the latter state is observed on the crystalline ice surface. When chemisorbed ozone is covered by an amorphous film, a temperature increase above 60 K leads to diffusion (with a weak yield) of ozone in the water lattice. Absorbed ozone remains in the ice bulk until sublimation of the ice film near 155 K.

I. Introduction

During the past decade, several studies have used temperature-programmed[1−4] spectroscopy and vibrational spectroscopy[5−16] to characterize the interaction of specific atmospheric species with a water ice surface. Interest in the subject was mainly motivated by the role of stratospheric heterogeneous chemistry in polar stratospheric clouds, which plays an important role in polar ozone depletion. Reflection−absorption IR spectroscopy (RAIRS) is a powerful method for studying reactivity at surfaces and in the ice bulk. However, it needs ultrathin ice films under UHV in order to investigate both surface and bulk phenomena with a low sublimation rate of the films.[17] Although these conditions are not quite the same as those encountered in polar stratospheric clouds of type II consisting of ice which condenses below 187 K, the fundamental bands of molecules adsorbed on the surface or absorbed within ice multilayers can provide information about direct surface/adsorbate interaction as well as about the structural nature of the multilayers, with the possibility of identifying intermediates and reaction products. As for examples, RAIRS has been used to study the interactions of HCl,[8−10] HBr, HI,[10] N_2O_5,[9,11] $ClONO_2$,[12,13] and CH_3COCH_3[14] with ice as well as their photochemical behaviors in the condensed phases of Cl_2O, Cl_2O_2[15], and OClO.[16] Furthermore, results can be of interest for the surface chemistry of ice and of molecular solids in particular in astrophysics where water ice is most abundant in celestial bodies such as comets, satellites of the outer planets, and icy ring particles.

This paper presents the first spectroscopic characterization of neat ozone (amorphous and crystalline phases) and of ozone adsorbed on ice films deposited on a side of a gold plated cube. Interaction of ozone with a water ice surface was studied on two types of ices: amorphous ice deposited from water vapor below 100 K and crystalline ice deposited from water vapor at 155 K then cooled at 55 K. We give evidence for two distinct states of ozone on an amorphous ice surface: a physisorbed state and a chemisorbed state related to ozone trapped in the micropores. Only the physisorbed state is observed on a crystalline surface. The temperature increase of amorphous water sandwich layers shows that a small amount of ozone remains in the bulk and desorbs only when water sublimes.

II. Experimental Section

The experiments were performed using a rotatable closed cycle helium refrigerator (Air Product, Displex 202 A), which was pumped continuously (10^{-7} mbar background pressure range). Thin films of ice were produced upon a thermostated gold side of a substrate cube. The temperature of the metal substrate (10 to 170 K) was controlled by a silicon diode (Scientific Instruments 9600−1). Water was deionized, triply distilled, and then degassed by freeze−thaw cycles under vacuum before use. Water layers were grown from water vapor via a capillary connected to a pulsed dosing system, which provides pulses of gas during 2 ms at a frequency of one pulse per two seconds leading to a deposition rate of about 2×10^{-3} mmol h^{-1}. Typical ice films thicknesses were less than 500 nm. Ozone was prepared from natural oxygen (Air Liquide N50) contained in a glass vacuum finger excited by a Tesla coil discharge with trapping of ozone at liquid nitrogen temperature. Residual oxygen was removed by freeze−pump−thaw cycles with liquid nitrogen.

Initially, ozone was directly deposited at low pressure (10^{-7} mbar) via a capillary. However, results showed that only part of the ozone was condensed on the substrate, the other part condensing very slowly over several hours after the gate valve was closed. On the basis of these observations, ozone was codeposited above 30 K with helium as carrier gas, a technique that prevented the above effect. The initial mixture was typically O_3/ He = 1/25 with a total pressure of helium of 150 Torr. Gas was deposited via a capillary with a rate of 3 mmol h^{-1}. The deposition nozzle parameters were 1 mm inner diameter and a distance of 20 mm from the cold substrate. Using two sides (at 180°) of our rotatable gold cube substrate, it was possible, in each experiment, to compare the spectrum of ozone directly deposited on the substrate and the spectrum of ozone deposited on water ice in the same experimental conditions. Care was taken (with proper collimation of the pulsed nozzle beam and

* To whom correspondence should be addressed.
† Laboratoire Associé à l'Université P. et M. Curie.

10.1021/jp0008290 CCC: $19.00
Published on Web 07/08/2000

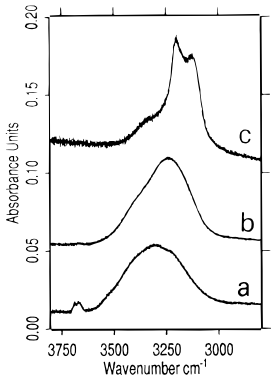

Figure 1. Typical infrared OH− stretching spectra of water ice films deposited on a gold cube at different temperatures: (a) deposition at 11 K (high-density amorphous ice), (b) deposition at 70 K (low-density amorphous ice), (c) deposition at 155 K (crystalline ice).

checking the residual when no deposit was done) to have a real blank (O_3 without H_2O) on one side and the sample to be studied (ozone on ice) on the other side. The infrared measurements were made in the reflection/absorption geometry with an incidence angle of 5° to the surface normal using a Bruker 113v spectrometer. Spectra were recorded at 0.5 and 2 cm^{-1} nominal resolutions from co-addition of 100 interferograms.

III. Results and Discussion

1. Water Ice Films. From electron diffraction, Jenniskens[18] showed that, at low pressure and temperature, water ice, which is formed by vapor deposition, exists in three metastable amorphous forms and two crystalline forms. Below 30 K, ice forms a high-density amorphous form (I_{ah}, 1.1 g cm^{-3}) which evolves gradually into a low-density amorphous form (I_{al}, 0.94 g cm^{-3}) over the 38 to 68 K temperature range. Above 130 K, ice forms another amorphous phase (I_{ar}), which coexists with the cubic crystalline form up to 200 K. The recrystallization of cubic to hexagonal ice occurs above 200 K when a gradual 1 K min^{-1} warming after deposition at 15 K is performed. Amorphous ice below 100 K is very porous. In particular, the term "high density" ice refers to the compact bulk density of ice. In the presence of micropores, the density changes and can reach values less than 0.75 g cm^{-3}.[19] Thus, vapor deposited ice may reach a specific surface area of the order of 200 m^2 g^{-1}.[20] Studies of N_2 and Ar adsorption measurements at 77 and 87 K showed a porous structure of ice with a wide pore size distribution (10 Å to 30 Å of radius) depending on both temperature and condensation rate.[21] Recently, by X-ray diffraction of krypton layers on the amorphous ice formed by vapor deposition in the 13−45 K temperature range, micropores with a diameter of 15 Å-20 Å, and a volume of 0.045 cm^3 g^{-1} were found.[22]

Numerous infrared spectroscopic studies have been reported in order to investigate the structural differences of the various water ice forms. Transmission mode was used[23−26] as well as reflection absorption at grazing incidence angle.[27,29] With our actual configuration (Fourier transform infrared reflection with an incidence angle of 5°) due to the metal surface selection rules, only the transversal optical mode with a transition dipole moment parallel at the surface can be excited.[30] A thorough description of water absorption including characterization of multilayers phases under our experimental conditions appears elsewhere.[31] Figure 1 compares some typical spectra of water in the ν_{OH} region obtained at different deposition temperatures. Thin films of high-density amorphous ice at 11 K show submaxima, whose number and frequencies depend on deposition conditions, and narrow bands between 3670 and 3700 cm^{-1} due to non-hydrogen-bonded OH of ice clusters of different sizes. Amorphous, low-density ice is characterized by a well reproducible ν_{OH} band at about 3250 cm^{-1}. In our configuration, due perhaps to reorientation effects, dangling bands at 3699 cm^{-1} characterizing the surface[29,32] are not observed. Above 150 K, the ν_{OH} band is characterized by two bands measured at about 3200 and 3130 cm^{-1} with a shoulder at 3380 cm^{-1} indicating that some parts of the films stay as I_{ah}.

Two important observations were made and deserve attention. Gradual transformation of high-density amorphous ice deposited at 11 K into low-density amorphous ice from 40 to 70 K is accompanied by an enhancement in the intensity of the ν_{OH} coupled band due to disappearance of disorder and formation of OH···O bonds. Transition time for complete transformation depends on the morphology and initial thickness of the high-density ice film. An increase in intensity of the ν_{OH} band was also observed when helium or pure ozone were deposited on the surface of low-density amorphous ice. This behavior reflects the degree of porosity and the defects of the bulk. New vacancies can be formed and density of water ice decreases.

2. Neat Solid Ozone. Only one earlier study of the IR spectrum of solid ozone deposited at 30 K has been reported briefly by P. Brosset et al. as part of their studies of O_3 in inert matrices.[33] The ν_3 asymmetric stretching mode, the most intense, was characterized by a broad band of full width at half-maximum (fwhm) of 10.2 cm^{-1} centered at 1037.0 cm^{-1}. The ν_2 bending mode and the ν_1 symmetric stretching mode were located at 703.9 and 1108.8 cm^{-1}, respectively. In fact, the spectrum of solid ozone is dependent on deposition techniques, the temperature, and the history of the sample as illustrated in Figure 2 in the ν_3 and ν_2 regions of ozone for: (i) fast direct deposition of ozone at 11 K; (ii) deposition of an ozone/argon mixture at 20 K followed by annealing at 40 K for obtaining ozone layers with all argon evaporated; (iii) deposition of an ozone/helium mixture at 30 K (a temperature preventing trapping of He) or slow direct deposition of ozone; (iv) direct deposition of ozone, ozone/helium, or ozone/argon mixtures at 55 K. When ozone is deposited rapidly at 11 K or with argon as carrier gas at 40 K, the ν_3 band is similar to that described in ref 33. It appears as a broad band located at 1037.1 cm^{-1} with a shoulder at 1043.0 cm^{-1} (fwhm = 9.1 cm^{-1}). At 55 K whatever the deposition technique, the ν_3 mode appears as a very narrow line (fwhm = 1.4 cm^{-1}) located at 1026.9 cm^{-1} with two weak satellites to 1048.0 and 1054.4 cm^{-1}. Between 30 and 55 K, the deposition of O_3 with He as carrier gas (or directly deposited) leads to an asymmetrical band centered at 1027.3 cm^{-1} with a shoulder toward high frequencies. These observations give evidence for the existence of two phases of ozone: an amorphous phase characterized by a broad ν_3 band at about 1037.1 cm^{-1} and a crystalline phase characterized by a narrow band centered at 1026.9 cm^{-1}.

Assignment of the two satellite bands observed at 1054.4 and 1048.0 cm^{-1} in the crystalline ozone is not straightforward. Their relative intensities in regard to the 1027.7 cm^{-1} absorption varied, in some cases, from one spectrum to another but showed the same behavior as the 1027.7 cm^{-1} band when temperature was increased indicating that they belong to a species containing at least one ozone molecule. These features are not due to aggregates between ozone and CO_2 (always present as traces in our spectra) as probed by subsequent experiments in which CO_2 was added to ozone. It could be suggested that the absorptions at 1054.4 and 1048.0 cm^{-1} belong to clusters of ozone formed in the gas phase. Ozone aggregates have not been yet identified in gas phase. In oxygen matrix, the ozone dimer

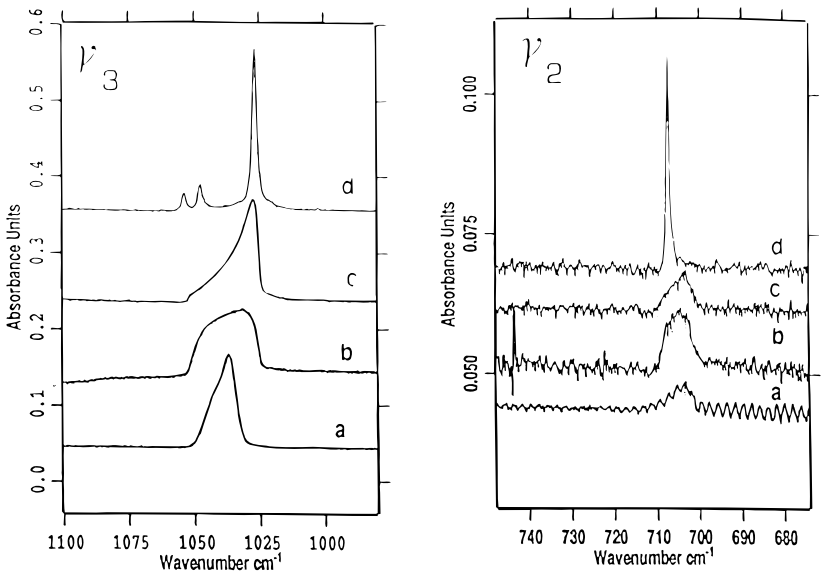

Figure 2. FTIR spectra of condensed films of ozone deposited on a gold substrate under various conditions: (a) deposition of pure ozone at 11 K, (b) deposition of an ozone-argon mixture (O_3/Ar = 1/50) at 20 K followed by annealing at 40 K, (c) deposition of an ozone-helium mixture at 30 K (O_3/He = 1/20), (d) deposition at 55 K of pure ozone or ozone with a carrier gas.

TABLE 1: Comparison with Gas Phase of Observed Vibration Frequencies (ν in cm^{-1}) and Full Width at Half-Maximum (fwhm in cm^{-1}) for Amorphous Ozone, Crystalline Ozone, and Ozone Trapped in Nitrogen Matrix

	ozone in gas	amorphous ozone		crystalline ozone		ozone in N_2 matrix	
	ν	ν	fwhm	ν	fwhm	ν	fwhm
ν_1 (A_1)	1103.1[a]	1106.1	5.8	1107.1	3.8	1108.3[a]	0.5
ν_2 (A_1)	700.9[a]	703.5	4.6	707.6	0.5	704.2[a]	1.1
ν_3 (B_1)	1042.1[a]	1037.1	9.1	1026.9	1.4	1042.8[a]	0.4
$\nu_1 + \nu_3$	2110.7[a]	2110.1	11.4	2108.6	9.3	2117.1[a]	1.4
$3\nu_3$	3046.1[b]			3033.9	3.4	3051.4[a]	0.9

[a] Reference 36. [b] Reference 33.

is characterized in the ν_3 region by two bands, one the most intense, at higher frequency than the monomer band, the other one at lower frequency; higher ozone aggregates produced absorptions blue shifted by 6 cm^{-1} from monomer band.[34] In solid ozone the large blue shift of the satellite bands from the characteristic band of amorphous ozone (wavenumbers higher than the value of ozone monomer in gas phase) poses a problem and the assumption that bands at 1054.4 and 1048.8 cm^{-1} are due to condensed ozone clusters is very problematic. Hence at this stage, no firm argument allows us to identify these satellite bands.

Table 1 compares the frequencies of amorphous and crystalline solid ozone with frequencies of ozone isolated in a nitrogen matrix and in gas phase. The band characteristic of the ν_1 mode is similar for amorphous and crystalline solid ozone (ν_1 = 1106.1 cm^{-1}, fwhm = 5.8 cm^{-1}), while for the ν_2 mode the peak for amorphous ice is located at 703.5 cm^{-1} with a fwhm of 4.6 cm^{-1} and the corresponding band for crystalline ozone appears as a narrow feature (fwhm = 0.5 cm^{-1}) located at 707.6 cm^{-1}. The ($\nu_1 + \nu_3$) combination was observed at about 2109 cm $^{-1}$ for all the samples. The $3\nu_3$ mode was observed as a sharp band at 3033.9 cm $^{-1}$ only in crystalline ozone. The ratio of $\nu_3/\nu_2/\nu_1$ was found to be 100/1.7/0.45 in amorphous ozone and 100/5.1/2.9 in crystalline ozone indicating that the crystallinity of ozone was also producing by a pronounced change in the relative intensity of individual absorptions bands. The intensity ratios differ from those observed in the gas phase[35,36] ($\nu_3/\nu_2/\nu_1$ = 100/ 4.2/ 3.8) and in argon or nitrogen matrices ($\nu_3/\nu_2/\nu_1$ = 100/ 0.54/ 7.7).[36]

Above 40 K, the lower subcomponent of the amorphous ozone ν_3 band disappeared but a contribution from amorphous ozone remained up to 50 K as a broad shoulder of the crystalline ozone ν_3 absorption then sublimated at 55 K without exhibiting a significant gradual transformation of amorphous to crystalline ozone. Crystalline ozone sublimated at higher temperature from 61 to 68 K. Kinetic studies of the desorption of crystalline ozone were performed at 61, 62, 63, and 65 K. A zero order expression was in agreement with the data as shown in Figure 3A. Such a kinetic order are generally observed for sublimation of a three-dimensional phase.[1,2] The logarithm of the sublimation rates varied linearly with reciprocal temperature (Figure 3B) and the activation energy for sublimation of neat crystalline ozone was deduced from the slope of such a plot. We determine $E_{a,sub}$ to be (23 ± 2.0) kJ mol^{-1}.

3. Interaction of Crystalline Ozone with Water Surfaces. Figure 4 shows typical spectra obtained by exposing a thin ice film at 55 K to increasing amounts of ozone. At this temperature, ozone exists as crystalline form. At very low surface coverage, there are two bands of approximately equal intensity observed in the ν_3 region of ozone. One band is at 1027.8 cm^{-1} and the other one at 1033.7 cm^{-1}. They characterize two states of ozone on the surface designated by α O_3 and βO_3 respectively. In the ν_{OH} region of water, the broad coupled ν_{OH} band increases in intensity and a new band appears at 3641.0 cm^{-1}. When the surface coverage is increased, the 1033.7 cm^{-1} and the 3641.0 cm^{-1} bands grow in concert, except for subsequent higher exposures of ozone, they keep the same intensity and only the 1027.8 cm^{-1} grows indicating formation of ozone multilayers which overlap the α state of ozone. Further experiments showed that the yield of β ozone depended on the ice morphology and on the deposition temperature. When ozone was deposited below 40 K, the 3641.0 cm^{-1} feature associated with β ozone did not

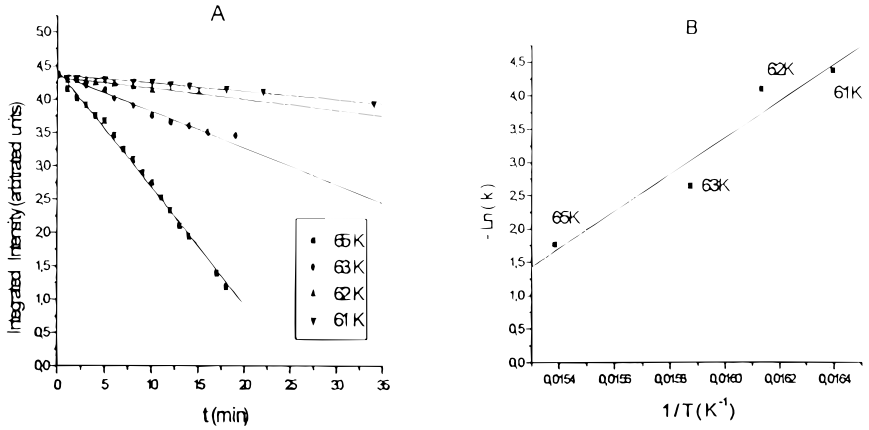

Figure 3. (A) kinetic curves for pure ozone desorption at 61, 62, 63, and 65 K. The integrated intensity of the ν_3 ozone band is plotted versus time for each temperature. (B) Arrhenius plots of ln(k) versus 1/T. The rate constant k is extracted from the slopes of the curves in Figure 3A.

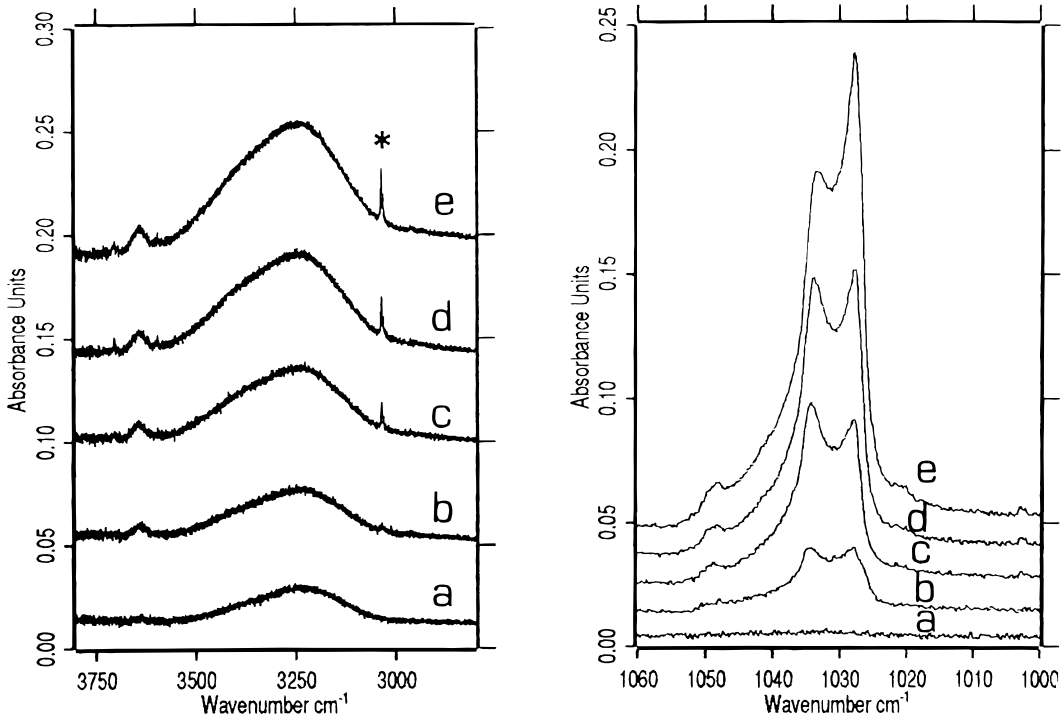

Figure 4. IR spectra at 55 K in the ν_{OH} region of water and in the ν_3 region of ozone obtained after exposing a water film to the same pressure of ozone during different times (a) 0, (b) 12, (c) 20, (d) 25, and (e) 30 min (*3 ν_3 band of ozone).

appear in the ν_{OH} region and only the asymmetric band of amorphous ozone was observed in the ν_3 region of ozone. At 60 K when amorphous ice was more ordered and less porous, the two associated bands at 3641.0 and 1033.7 cm^{-1} were very weak and when ozone was deposited on crystalline ice, the spectrum was a single superposition of the corresponding crystalline O_3 and water spectra.

These results show that α ozone is derived from a physisorbed state, while β ozone is derived from a molecular adsorbed state due to interaction between ozone and a free OH bond in H_2O, which is shifted to 3641.0 cm^{-1} at 55 K. The frequency of the ν_3 stretch in β ozone is 7 cm^{-1} below that in condensed ozone consistent with hydrogen bonding formation. The β ozone state results probably from trapping of ozone in the micropores of amorphous ice, for two reasons: (i) on a crystalline ice film in which all pores are collapsed, no contribution of a perturbed free OH bond (expected to form at the corresponding surface) is observed, and (ii) the β O_3 yield depends on the porosity of amorphous films and requires a temperature higher than 35 K to be formed. Conversely, the α state appears independent of the presence of free OH groups at the ice surface and intermolecular forces between O_3 and the smooth surface are quite weak as one might expect from the structure of the one to one complex between O_3 and H_2O isolated in an argon matrix[37] and in the gas phase.[38] In solid argon, the 1:1 complex is characterized by a blue shift of 3.3 cm^{-1} in the ν_3 absorption of ozone and a red shift of 8 cm^{-1} in the ν_3 absorption of water. Interaction occurs mainly by bonding between the oxygen atom of the water molecule and an oxygen atom of ozone. However, force field calculations indicate a non equivalence of the two OH water oscillators suggesting an orientation allowing a very weak hydrogen bond of the type HOH···O_3. These results were confirmed by microwave studies associated with ab initio calculations[38] which showed that water and the central oxygen atom of ozone were located in the *a*,*c* plane of the complex with a hydrogen atom oriented toward the terminal O atom of ozone establishing a very weak hydrogen bonding leading to a stabilization energy of 0.7 kcal mol^{-1}. From these earlier studies,[37,38] it seems reasonable to consider that orientation of α ozone on the smooth ice surface is nearly similar to that

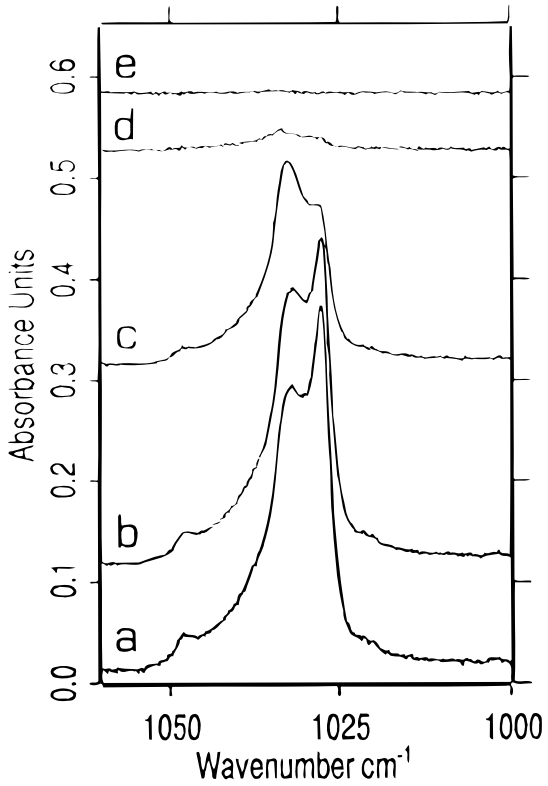

Figure 5. Annealing effects on the ν_3 band of ozone after deposition at 55 K of ozone on a water ice surface: (a) after deposition at 55 K; (b), (c), (d), and (e) after annealing at 63, 65, 67, and 70 K, respectively.

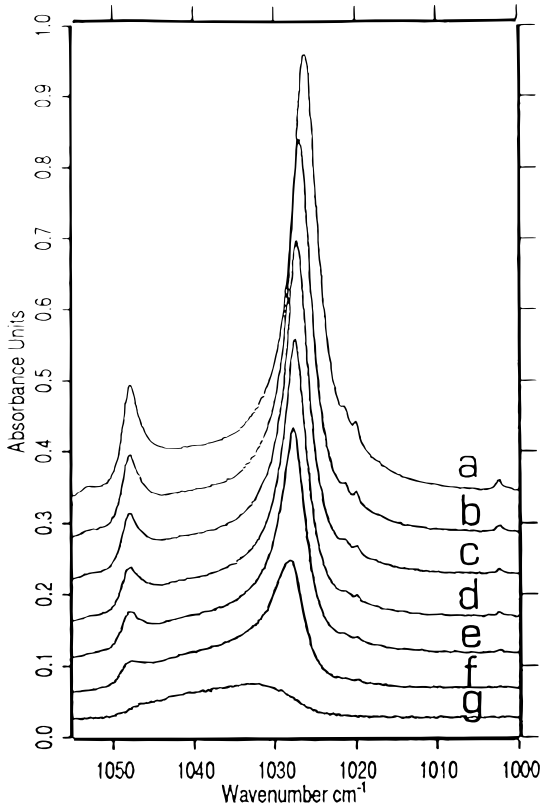

Figure 6. Spectral changes with time at 63 K in the ν_3 region of ozone after deposition of ozone at 63 K on a water ice surface: (a) 0, (b) 20, (c) 26, (d) 33, (e) 38, (f) 40, and (g) 180 min.

observed in the 1:1 $H_2O:O_3$ complex. Thus, ozone interacts weakly with oxygen atoms of water and not with the OH dangling bands of the geometrical surface.

A different situation occurs when ozone is trapped in sites of the bulk associated with pores in the lattice, this trapping occurring from diffusion of α ozone above 35 K. Because of cooperative factors created by water molecules surrounding ozone, the hydrogen bond between O_3 and water can be reinforced and better oriented. In argon matrix, higher aggregates than the 1:1 $H_2O:O_3$ complex were also identified by shifts in the infrared absorption of water.[37] In the $H_2O:(O_3)_2$ complex, the ν_3 asymmetric stretching of water was red shifted by 30 cm^{-1} and in large excess of water an absorption at 3620 cm^{-1} was observed in the ν_3 region of water. Thus, the frequency of water OH bond complexed by ozone in the pores (β ozone) located at 3641 cm^{-1} is in agreement with formation of an hydrogen bond between ozone and a water molecule coordinated to three other water molecules.

To gain insight into the nature of the interaction between ozone and water and into the possibility of migration of ozone in the bulk, three sets of experiments were performed for testing temperature effects on ozone deposited on water. In the first set, the temperature of a sample containing β ozone and α ozone overlapped with condensed ozone was increased from 55 to 70 K at a rate of 2 K min^{-1}. As illustrated in Figure 5, condensed ozone and β ozone desorbed for temperatures above 63 K but with a larger yield for condensed ozone between 63 and 65 K indicating a slightly higher activation energy for β ozone desorption than for condensed ozone, a behavior consistent with a process involving scission of the hydrogen bond between ozone and an OH bond in water. At 70 K, β ozone was totally desorbed as indicated by the disappearance of the 1033.7 cm^{-1} band with in parallel that of the 3641.0 cm^{-1} (not represented). Unfortunately, due to the overlap of bands characterizing the β, α states and multilayers of ozone and the weakness of the associated OH bond at 3641.0 cm^{-1} it was not possible to obtain kinetic curves and hence to determine accurately the activation energy or the desorption of the β and α states of ozone.

In the second set of experiments, a sample of multilayers of ozone deposited on a water film was kept at 63 K during several hours. After 1 h the major part of the ozone was desorbed but (Figure 6) an asymmetric weak band remained at 1033.1 cm^{-1} without a counterpart at 3641.0 cm^{-1} in the ν_{OH} region. This band diminished with a temperature increase but it disappeared totally only at 150 K. Although the frequency of this band is close to that characterizing the β state of ozone at the surface of micropores, it cannot be assigned to this species, which is desorbed at 70 K but rather to ozone trapped in the bulk. In this experiment, migration of ozone from the surface into the film, which occurs above 60 K, is in competition with desorption.

A third set of experiments which consisted of a study of the evolution of "amorphous water sandwich layers" with temperature confirmed the thermal diffusion of ozone in the bulk due to defects and inhomogeneities in the bulk as well as the insertion of ozone in the water lattice. Sandwich layers were formed by absorbing O_3 on a water ice film at 60 K then depositing a second water film on top of the ozone layer. As illustrated in Figure 7A when the second film of water was deposited on ozone, drastic changes occurred: the 3634.4 cm^{-1} band increased, while the narrow band at 1027.7 cm^{-1} characteristic of condensed crystalline ozone transformed into a broad band at 1033.8 cm^{-1} . After a night at the same temperature (60 K), only the band at 1033.8 cm^{-1} was observed with, in parallel, a weak decrease in intensity of the OH associated feature. At this stage, the film was annealed at 168 K at a rate of 5 K min^{-1} and successive spectra were recorded

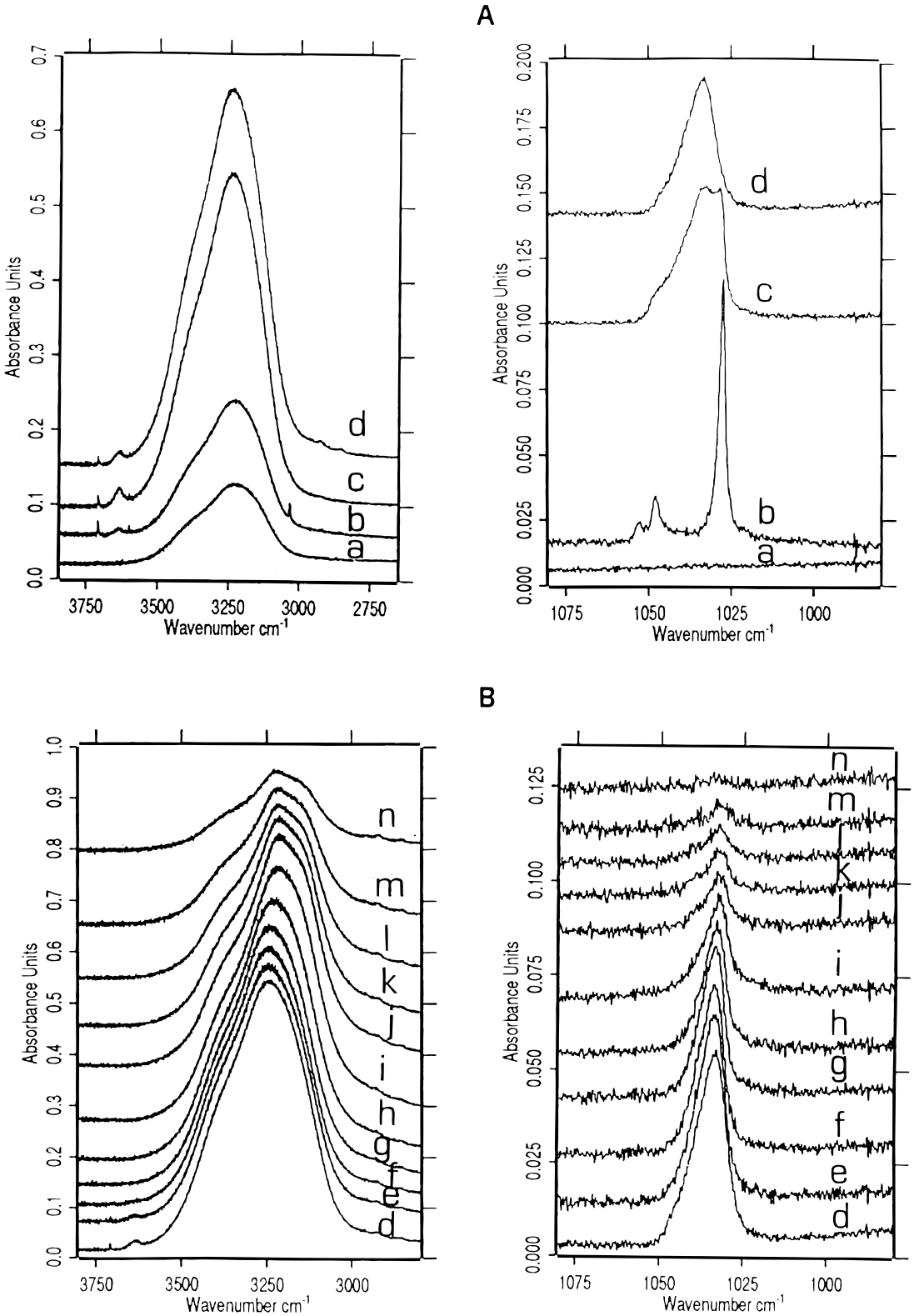

Figure 7. [A] IR spectra in the 3800−2800 cm^{-1} and in 1080−980 cm^{-1} regions for (a) pure water ice film deposited at 60 K, (b) water film exposed to ozone at 60 K, (c) film (b) after deposition of a second water layer at 60 K, (d) film (c) after a night at 60 K. [B] Spectral changes with temperature of the sample (d) (d) 60K, (e) 75 K, (f) 100 K, (g) 130 K, (h) 140 K, (i) 150 K, (j) 155 K, (k) 158 K, (l) 160 K, (m) 162 K, (n) 168 K.

at approximatively 5 K intervals. For each temperature step the samples were kept during 6 min and no change was observed. Some representative spectra in the ν_{OH} water and in the ν_3 ozone region are given in Figure 7B. From 60 to 75 K, no change was observed. From 80 to 100K, a decrease in intensity of the 1033.8 cm^{-1} absorption was observed with, in parallel, a decrease in intensity of the perturbed dangling band at 3634.4 cm^{-1}. This latter band disappeared at 100 K while the band of ozone remained unchanged from 100 to 130 K. At 140 K, the ozone absorption diminished again and disappeared at 168 K. In the 150−168 K temperature range, the ν_3 ozone band became more symmetric, it shifted to 1032.8 cm^{-1} and its disappearance

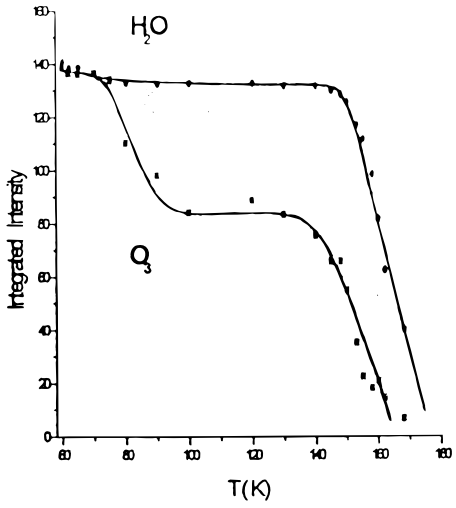

Figure 8. Integrated intensities of the ν_{OH} band of water and of the ν_3 band of ozone versus temperature for the spectra in Figure 7 B. Intensities of the latter band were multiplied by 220 to make them comparable to the ν_3 OH intensities. Lines are intended to guide the eye and do not represent a fit to the data.

was accompanied by the evaporation of water as evidenced by the decrease in intensity of the ν_{OH} coupled band. All these observations are well illustrated in Figure 8, which compares the integrated intensity versus temperature of the ν_3 ozone band with the integrated intensity of the water ν_{OH} absorption. Results show that the band observed in the ν_3 ozone region corresponds, in fact, to different states of ozone in the bulk: one to ozone trapped into defects in the lattices (grain boundaries, micropores) and another to ozone trapped in the water bulk. When the temperature is increased, there is competition between release of ozone trapped in the pores and diffusion in the lattice. Between 75 and 100 K, the pores tend to collapse and β ozone is released as indicated by the disappearance of the feature at 3634.4 cm^{-1} and the decrease in intensity of the 1033.8 cm^{-1} band. This latter absorption, which is still present at 100 K, can be assigned to ozone molecules inserted in the lattice and disturbing the long range network of tetrahedracally coordinated pure water. At 130 K when amorphous ice transforms into cubic ice, part of the ozone is squeezed out, the transformation of ice resulting in the opening of channels that allow release of ozone. The small amount of ozone, which is still trapped in the cubic ice, starts at 150 K when water itself evaporates. The mutual evaporation of both water and ozone at a nearly same rate is consistent with an assignment of ozone associated with an absorbed bulk state and could even suggest formation of a local ozone clathrate hydrate. Release of ozone with temperature which probes the gradual transformation of water is similar to previous findings for release of CH_4, Ar, N_2, Ne, and H_2[39] and CO.[39,40] In particular, the curve of Figure 8 is essentially the curve reported in Figure 9 of ref 40 for the temperature dependence of the 2138 cm^{-1} band of CO deposited on ice.

To determine if ozone penetrates into the bulk from the crystalline ice surface, the second set of experiments described above were repeated with ice previously annealed at 155 K and cooled to 63 K. In this case, ozone is totally desorbed from the surface and no band remained after several hours, indicating that diffusion of ozone into the bulk occurs only from the β O_3 state and not from the physisorbed α state. Furthermore, when mixtures of ozone and water were deposited at 150 K, only the spectrum of water was observed while the heating of similar mixtures deposited at 30 K led to the same results as those obtained by temperature effects on the double-layered sample as described in details in a forthcoming paper.[41] Thus, in stratospheric conditions, ozone is not transported to water ice and hence it cannot react with other adsorbed species.

Conclusions

Infrared spectra of solid ozone and ozone deposited on amorphous and crystalline water ice surfaces are reported. Two distinct states of ozone at the ice surface have been chatacterized: a physisorbed state (O_3 α state) and a chemisorbed state (O_3 β state) that is unique to amorphous ice. The spectral properties of the α ozone state are those of pure ozone. The β state which is associated with ozone interacting with the hydrate surface of micropores via a hydrogen bond is characterized by two bands located at 3641.0 cm^{-1} at 55 K in the ν_{OH} water region and at 1033.8 cm^{-1} in the ν_3 ozone region. Above 60 K, there is a weak incorporation of ozone into the lattice structure from a pathway involving the β state. Ozone which remains in the lattice until sublimation of the ice film near 155 K is characterized by a band at 1032.8 cm^{-1} without a counterpart in the ν_{OH} region. The absence of diffusion of ozone from the crystalline ice surface implies that the coverage of adsorbed ozone under stratospheric conditions is insignificant. Furthermore, a mixture of water and ozone deposited at 150 K shows that ozone is not trapped in the ice bulk. Thus, despite the dynamical character of the polar stratospheric surface, the constant flux of water molecules which constantly desorbs and recombines cannot trap ozone. These results are consistent with the laboratory measurements of direct ozone loss on an ice surface over the temperature 195 to 262 K using a flow tube reactor reported by Dlugokencky and Ravishankara.[42] Interaction of ozone with amorphous ice which is characterized by the chemisorption of ozone in the pores followed by diffusion in the bulk is in agreement with the recent detection of ozone trapped in ice on Ganymede and on Saturn's satellites Rhea and Dione.[43,44] On these icy satellites, amorphous ice can act as a reservoir to keep ozone (produced from oxygen) at temperature exceeding its normal sublimation point in a vacuum.

Acknowledgment. This work was partly supported by PNCA (Program National de Chimie Atmosphérique) and PNP (Program National de Planétologie). We are grateful to Dr. C. Camy-Peyret (Director of the LPMA) who was very supportive of our experiments on ice films and performed a careful reading of the manuscript.

References and Notes

(1) Graham, J. D.; Roberts, T. J. *J. Phys. Chem.* **1994**, *98*, 5974.
(2) Blanchard, J. L.; Roberts, J. T. *Langmuir* **1994**, *10*, 3303.
(3) Graham, J. D.; Roberts, T. J.; Brown, L. A.; Vaida, V. *J. Phys. Chem.* **1996**, *100*, 3115.
(4) Isakson, M. J.; Sitz, G. O. *J. Phys. Chem, A.* **1999**, *103*, 2044.
(5) Buch, V.; Delzeit, L.; Blackledge, C.; Devlin, J. P. *J. Phys. Chem.* **1996**, *100*, 3732.
(6) Givan, A.; Loewenschuss, A.; Nielsen, C. J. *J. Chem. Soc., Faraday Trans.* **1996**, *92*, 4927.
(7) Loewenschuss, A.; Givan, A.; Nielsen, C. J. *J. Mol. Struct.* **1997**, *408*, 533.
(8) Graham, J. D.; Roberts, J. T. *Geophys. Res. Lett.* **1995**, *22*, 251.
(9) Koch, T. G.; Banham, S. F.; Sodeau, J. R.; Horn, A. B.; McCoustra, M. R. S.; Chesters, M. A. *J. Geophys. Res.* **1997**, *102*, 1513.
(10) Barone, S. B.; Zondlo, M. A.; Tolbert, M. A. *J. Phys. Chem. A* **1999**, *103*, 9717.
(11) Horn, A. B.; Koch, T. G.; Chesters, M. A.; McCoustra, M. R. S.; Sodeau, J. R. *J. Phys. Chem.* **1994**, *98*, 946.
(12) Sodeau, J. R.; Horn, A. B.; Banham, S.F.; Koch, T. G. *J. Phys. Chem.* **1995**, *99*, 6258.
(13) Barone, S. B.; Zondlo, M. A.; Tolbert, M. A. *J. Phys. Chem. A* **1997**, *101*, 8643.
(14) Schaff, J. E.; Roberts, J. T. *J. Phys. Chem.* **1994**, *98*, 6900.

(15) Gane, M. P.; Williams, N. A.; Sodeau, J. R. *J. Chem. Soc., Faraday Trans.* **1997**, *93*, 2747.
(16) Graham, J. D.; Roberts, J. T.; Anderson, L. D.; Grassian, V. H. *J. Phys. Chem.* **1996**, *100*, 19551.
(17) Haynes, D. R.; Tro, N. J.; George, S. M. *J. Phys. Chem*. **1992**, *96*, 8502.
(18) Jenniskens, P.; Blake, D. F. *Science* **1994**, *265*, 753.
(19) Brown, D. E.; George, S. M.; Huang, C.; Wong, E. K. L.; Rider, K. B.; Smith, R. S.; Kay, B. D. *J. Phys. Chem.* **1996**, *100*, 4988.
(20) Ghormley, J. A. *J. Chem. Phys.* **1967**, *46*, 1321.
(21) Schmitt, B.; Ocampo, J.; Klinger, J. *J. Phys.* **1987**, *48*, C 1−519.
(22) Langel, W.; Fleger, H. N.; Knözinger, E. *Ber. Bunsen-Ges. Phys. Chem.* **1994**, *98*, 81.
(23) Hagen, W.; Tiellens, O. M.; Greenberg, J. M. *Chem. Phys.* **1981**, *56*, 367.
(24) Delzeit, L.; Devlin, J. P.; Buch, V. *J. Chem. Phys.* **1997**, *107*, 3736.
(25) Givan, A.; Loewenschuss, A.; Nielsen, C. J. *J. Phys. Chem. B.* **1997**, *101*, 8696.
(26) Buch, V.; Devlin, J. P. *J. Chem. Phys.* **1999**, *110*, 3437.
(27) Jenniskens, P.; Banham, S. F.; Blake, D. F.; McCoustra, M. R. S. *J. Chem. Phys.* **1997**, *107*, 1232.
(28) Horn, A. B.; Banham, S. F.; McCoustra, M. R. S.*J. Chem. Soc., Faraday Trans.* **1995**, *91*, 4085.
(29) Zondlo, M. A.; Onash, T. B.; Warhawsky, M. S.; Tolbert, M. A.; Mallick, G.; Arentz, P.; Robinson, M. S. *J. Phys. Chem. B* **1997**, *101*, 10887.
(30) Greenler, R. G. *J. Chem. Phys.* **1966**, *44*, 310.
(31) Schriver-Mazzuoli, L.; Schriver, A. *J. Mol. Struct.* **2000**. In press.
(32) Callen, B. W.; Griffiths, K.; Norton, P. R. *Surf. Sci. Lett.* **1992**, *261*, 144.
(33) Brosset, P.; Dahoo, R.; Gauthier-Roy, B.; Abouaf-Marguin, L. *Chem. Phys.* **1993**, *172*, 315.
(34) Schriver-Mazzuoli, L.; de Saxcé, A.; Lugez, C.; Camy-Peyret, C.; Schriver, A. *J. Chem. Phys.* **1995**, *102*, 690.
(35) Flaud, J. M.; Camy-Peyret, C.; Rinsland, C. P.; Smith, M. A. H.; Malathy Devi, V. *Atlas of Ozone Parameters from Microwaves to Medium Infrared*; Academic Press: New York, 1990.
(36) Schriver-Mazzuoli, L.; Schriver, A.; Lugez, C.; Perrin, A.; Flaud, J. M. *J. Mol. Spectrosc.* **1996**, *85*, 176.
(37) Schriver-Mazzuoli, L.; Barreau, C.; Schriver, A. *Chem. Phys.* **1990**, *140*, 419.
(38) Gilles, J. Z.; Gilles, C. W.; Suenram, R. D.; Lovas, F. T.; Schmidt, T.; Cremer, D. *J. Mol. Spectrosc.* **1991**, *146*, 493.
(39) Laufer, D.; Kochavi, E.; Bar-Nun, A. *Phys. Rev. B* **1987**, *36*, 9219.
(40) Givan, A.; Loewenschuss, A.; Nielsen, C. J. *Vib. Spectrosc.* **1996**, *12*, 1.
(41) Chaabouni, H.; Schriver-Mazzuoli, L.; Schriver, A. *Low-Temperature Physics.* (Special issue on matrix isolation.) **2000**. In press.
(42) Dlugokencky, E. J.; Ravishankara, A. R. *Geophys. Research Lett.* **1992**, *19*, 41.
(43) Noll, K. S.; Jonhson, R. E.; Lane, A. L.; Domingue, D. L.; Weaver, H. A. *Science* **1996**, *273*, 341.
(44) Noll, K. S.; Roush, J. L.; Cruikshank, D. P.; Jonhson, R. E.; Pendleton, Y. P. *Nature* **1997**, *388*, 45.